

Mesenchymal Stromal Cells: Inhibiting PDGF Receptors or Depleting Fibronectin Induces Mesodermal Progenitors with Endothelial Potential

S. G. BALL,^{a,b} J. J. WORTHINGTON,^b A. E. CANFIELD,^{a,c} C. L. R. MERRY,^d C. M. KIELTY^{a,b}

Key Words. Mesenchymal stromal cells • Spheroids • Platelet-derived growth factor receptor • Fibronectin • Endothelial • Neovascularization

^aWellcome Trust Centre for Cell-Matrix Research, ^bFaculty of Life Sciences, ^cFaculty of Medical and Human Sciences, and ^dStem Cell Glycobiology Group, School of Materials, Faculty of Engineering and Physical Sciences, University of Manchester, Manchester, Lancashire, United Kingdom

Correspondence: Cay Kielty, BSC.Hons, Ph.D., Wellcome Trust Centre for Cell-Matrix Research, University of Manchester, Manchester, Lancashire, U.K. Telephone: +44 161 275 5739; Fax: +44 161 275 5082; e-mail: cay.kielty@manchester.ac.uk

Received April 8, 2013; accepted for publication August 16, 2013; first published online in *STEM CELLS EXPRESS* September 10, 2013.

© AlphaMed Press
1066-5099/2014/\$30.00/0

<http://dx.doi.org/10.1002/stem.1538>

This is an open access article under the terms of the Creative Commons Attribution License, which permits use, distribution and reproduction in any medium, provided the original work is properly cited.

ABSTRACT

Realizing the full therapeutic potential of mesenchymal stromal/stem cells (MSCs) awaits improved understanding of mechanisms controlling their fate. Using MSCs cultured as spheroids to recapitulate a three-dimensional cellular environment, we show that perturbing the mesenchymal regulators, platelet-derived growth factor (PDGF) receptors or fibronectin, reverts MSCs toward mesodermal progenitors with endothelial potential that can potently induce neovascularization *in vivo*. MSCs within untreated spheroids retain their mesenchymal spindle shape with abundant smooth muscle α -actin filaments and fibronectin-rich matrix. Inhibiting PDGF receptors or depleting fibronectin induces rounding and depletes smooth muscle α -actin expression; these cells have characteristics of mesenchymoangioblasts, with enhanced expression of mesoderm and endoderm transcription factors, prominent upregulation of E-cadherin, and Janus kinase signaling-dependent expression of Oct4A and Nanog. PDGF receptor-inhibited spheroids also upregulate endothelial markers platelet endothelial cell adhesion molecule 1 and vascular endothelial-cadherin and secrete many angiogenic factors, and *in vivo* they potently stimulate neovascularization, and their MSCs integrate within functional blood vessels that are perfused by the circulation. Thus, MSC potency and vascular induction are regulated by perturbing mesenchymal fate. *STEM CELLS* 2014;32:694–705

INTRODUCTION

Fulfilling the potential of mesenchymal stromal (stem) cells (MSCs) in regenerative medicine requires an improved understanding of the mechanisms that control their fate. It is well known that, in adherent cultures, MSCs adopt a myofibroblast-like contractile phenotype and can differentiate along mesenchymal lineages in response to defined supplements [1, 2]. Less is known about MSCs *in vivo* and even the lineage specification of their embryonic precursors is ill-defined [3, 4]. MSCs occupy perivascular niches throughout the body [5] and in the bone marrow can undergo osteogenic differentiation and support hematopoiesis [6, 7]. Although MSCs can express endothelial markers *in vitro* in response to growth factors [8], or to cell density-dependent Notch signals [9], their ability to form functional vascular endothelium and contribute to new blood vessel formation *in vivo* remains uncertain. We report that MSC fate is changed by perturbing mesenchymal regulators, which in turn stimulates neovascularization and their integration into functional blood vessels.

MSCs are derived predominantly from the mesodermal lineage, but also from endoderm by epithelial-mesenchymal transition and from ectodermal neural crest [10–12]. During development, the mesoderm forms distinct mesenchymal and hemato-endothelial lineages. Using embryonic stem cells directed toward mesoderm, one group identified a common mesoderm-derived precursor for MSCs and endothelial cells, which they termed a mesenchymoangioblast [3, 4]. Others described a bone marrow mesodermal progenitor cell population with dual mesenchymal and endothelial differentiation potential [13]. These data point to a mesodermal cell stage with potential to form mesenchyme or endothelium.

Platelet-derived growth factor (PDGF) receptors (PDGFR) are markers and critical regulators of mesenchyme [14–16]. Knockout mice showed that loss of PDGFR α or PDGF-A disrupts mesenchymal tissue formation, whereas loss of PDGFR β disrupts pericytes and smooth muscle [17, 18]. Knockout of PDGFR α caused death of 50% of embryos before E10 and the rest shortly after birth [19], while in chick, signaling through PDGFR α was required for mesodermal cell migration [20]. We have shown that PDGFR signaling in

MSCs regulates migration, proliferation, and cytoskeletal organization, through RhoA/Rho kinase (ROK) signaling [21] and by cross-talk with fibronectin (FN)-activated integrin $\alpha 5\beta 1$ [22] and neuropilin-1 [23]. We showed that FN/ $\alpha 5\beta 1$ activates PDGFR β in the absence of PDGF growth factors, and is also required to potentiate PDGF-BB-mediated PDGFR β activation [22]. FN, a chordate innovation, is an extracellular adhesive glycoprotein [24], which controls the deposition of fibrillar matrices by mesenchymal cells [25], and thus tissue formation. FN-null mice are early embryonic lethal due to multiple cardiovascular defects [26]. PDGFR β signaling enhances FN expression [27], and together they are potent drivers of mesenchyme.

We have tested the hypothesis that disrupting mesenchymal regulators can alter the fate of human bone marrow-derived MSCs. Cell cytoskeleton was modified by inhibiting PDGFRs or by depleting FN, within three-dimensional (3D) spheroids. Resulting MSCs were rounded rather than spindle-shaped, with depleted smooth muscle α -actin (SMA) filaments and greatly reduced migratory capacity. They were mesenchymoangioblast-like with enhanced transcription factors such as EOMES, Foxh1, and Mixl1. These cells also exhibited marked upregulation of E-cadherin, Oct4A, and Nanog as well as endothelial markers platelet endothelial cell adhesion molecule 1 (PECAM-1) and vascular endothelial (VE)-cadherin and angiogenic growth factors. They had endothelial-like organization, and markedly enhanced neovascularization and integration into new functional blood vessels that were perfused by the circulation *in vivo*. Thus, perturbation of mesenchymal regulators modulates MSC fate and angiogenic potential *in vivo*. This discovery offers opportunities for therapeutic revascularization.

MATERIALS AND METHODS

Cell Culture and Spheroid Formation

Human bone marrow-derived MSCs from a 21-year-old female, and 21- and 33-year-old males (Lonza, Allendale, NJ, <http://www.lonza.com>), were subcultured on 0.1% gelatin, maintained in MesenPRO RS growth medium (Life Technologies, Grand Island, NY, <http://www.lifetechnologies.com>), and used at passage 5. Spheroids were formed by seeding 60,000 MSCs in growth medium \pm 0.1 μ M PDGFR inhibitor-IV (EMD Millipore, Billerica, MA, <http://www.emdmillipore.com>) [28], into individual wells of a low cell binding 96-well plate (Nunc 145399; Thermo Scientific, Waltham, MA, <http://www.thermofisher.com>) and cultured at 37°C for 5 days. Other small molecular inhibitors; EGFR (PD168393), FGFR (341608), VEGFR (ZM323881), Rho-kinase (H-1152), Rac1 (553508), MEK (PD98059), PI3K (LY294002), and JAK (Inhibitor I), were all obtained from EMD Millipore, Billerica, MA, <http://www.emdmillipore.com> and previously described [28].

Quantitative RT-PCR Analysis

For RNA isolation; ≥ 12 identically cultured spheroids were pooled together for analysis. RNA was isolated using Trizol reagent (Life Technologies, Grand Island, NY, <http://www.lifetechnologies.com>) followed by digestion with RNase-free DNase (Promega, Madison, WI, <http://www.promega.com>). First strand cDNA synthesis was performed using AMV reverse transcriptase (Roche, Basel, Switzerland, [\[com\]\(http://www.roche.com\)\), and real-time quantitative PCR using GoTaq qPCR kit \(Qiagen, Valencia, CA, <http://www.qiagen.com>\). Gene expression was determined relative to GAPDH using the \$\Delta\Delta C_t\$ method. All primer sequences are provided in Supporting Information Table S1.](http://www.roche-</p>
</div>
<div data-bbox=)

siRNA Knockdown

MSCs were transfected with 10 nM small interfering RNAs (siRNAs) using Lipofectamine RNAi MAX reagent (Life Technologies, Grand Island, NY, <http://www.lifetechnologies.com>), then cultured for 24 hours in the presence of the reagent and siRNA. Transfected MSCs were then trypsinized and used to form spheroids in the presence of fresh Lipofectamine reagent and siRNA which remained in the culture at 37°C for 5 days. Validated siRNAs were used to knockdown FN (1027417) (Qiagen, Valencia, CA, <http://www.qiagen.com>); scrambled siRNA (Qiagen, Valencia, CA, <http://www.qiagen.com>) was used as a control.

Immunoblotting

For protein isolation; ≥ 12 identically cultured spheroids were pooled together for analysis. Protein lysate isolation, immunoblotting, and quantification were performed as previously described [21]. Details of the antibodies used are given in Supporting Information Table S2.

Matrigel In Vitro Network and Implant Analysis

For network formation, spheroids were dissociated into single cells by incubation with 0.001% (wt/vol) collagenase type IV (Sigma Aldrich, St. Louis, MO, <http://www.sigmaaldrich.com>) in phosphate buffered saline for 1 hour at 37°C, followed by TrypLE Select (Life Technologies, Grand Island, NY, <http://www.lifetechnologies.com>) digestion for 10 minutes. MSCs were seeded onto growth factor reduced Matrigel (BD Biosciences, San Jose, CA, <http://www.bdbiosciences.com>) and incubated at 37°C. For implants, spheroids were covered with Matrigel and incubated at 37°C.

Matrigel Plug In Vivo Angiogenesis Assay

Spheroids suspended in 200 μ l growth medium and 500 μ l of growth factor reduced Matrigel were injected subcutaneously into the flanks of 6–8-week-old C57BL/6 mice. Five mice were each injected with 10 control spheroids and five with 10 PDGFR-IV spheroids. Two weeks after injection, mice were sacrificed, plugs removed, and immediately fixed in 4% (wt/vol) paraformaldehyde for 24 hours at 4°C, then incubated in 30% (wt/vol) sucrose solution for 24 hours at 4°C. Plugs were then embedded in OCT and 10 μ m sections obtained for immunofluorescence analysis which was performed as previously described [28].

To study whether new blood vessels were functional and integrated with the circulation, 200 μ l of 50 mg/ml FITC-dextran 2,000 kDa (Sigma Aldrich, St. Louis, MO, <http://www.sigmaaldrich.com>) was injected into the tail vein of mice, and allowed to perfuse for 10 minutes before the mice were sacrificed, and the plugs excised and processed, as above.

Whole Mount Immunofluorescence Analysis and Microscopy

Spheroids were prepared for confocal microscopy as described [29]. Details of the antibodies used are given in Supporting

Information Table S2. Images were collected on a Nikon C1 confocal using a TE2000 PSF inverted microscope, using $\times 60$ /NA 1.40 Plan Apo or $\times 20$ /NA 0.50 Plan Fluor objectives and $\times 3$ confocal zoom. Different sample images detecting the same antibodies were acquired under constant acquisition settings. Images were processed using Nikon EZ-C1 FreeViewer v3.3 software. Bright-field images were collected on an Olympus BX51 widefield microscope, using a $\times 10$ /NA 0.3 UPlan F1 objective. Images were captured with a CoolSNAP camera system and processed using MetaMorph imaging v5.0 software.

Statistical Analysis

Results are expressed as the mean \pm SD. Statistical differences between sets of data were determined using a paired Student's *t* test, with $p < .05$ considered significant.

RESULTS

PDGFRs regulate the formation of mesenchymal cells from mesoderm [14, 16]. These cells in turn make tissues by depositing and embedding themselves within a FN-rich extracellular matrix [24, 25]. FN/ $\alpha 5\beta 1$ is functionally linked with PDGFR β , both by activating PDGFR β in the absence of PDGF growth factors and by potentiating PDGF-BB-induced PDGFR β signaling [22]. Here, we used 3D spheroid cultures to test the hypothesis that cytoskeletal changes induced by inhibiting these functionally integrated mesenchymal regulators, PDGFR signaling and FN, revert MSCs toward a mesodermal progenitor with endothelial potential.

PDGFR Signaling Modulates MSC Spheroid Assembly and Organization

PDGFR signaling regulates the expression of contractile SMA filaments [14–16], which are not only a characteristic functional feature of vascular smooth muscle cells [30] but also abundantly expressed by MSCs [21], and are widely used as a distinctive mesenchyme marker. Using live cell imaging, we monitored the assembly of MSCs into control and PDGFR inhibitor-IV spheroids during the first 20 hours of formation (Supporting Information Video S1). While control MSC suspensions rapidly aggregated to form a spheroid, their assembly in the presence of PDGFR inhibitor-IV was markedly slower. After 6 hours of seeding, control MSCs formed a spheroid-like structure which contains a distinct outer ring of cells (Fig. 1A(i)); this feature was not detected during the assembly of PDGFR inhibitor-IV spheroids. After 20 hours of seeding, control MSCs formed a spherical structure (Fig. 1A(ii)), whereas PDGFR inhibitor-IV spheroids had a larger diameter but more flattened structure. These distinctive organizational features were maintained throughout a 5-day culture period (Fig. 1A(iii)); MSCs within control 3D spheroids retained their characteristic spindle-shaped morphology and expressed widespread abundant extended SMA filaments and FN (Fig. 1B(i)). However, MSCs within PDGFR inhibitor-IV spheroids were more rounded, and SMA and FN abundance were markedly reduced (Fig. 1B(ii)). Within the core of the spheroids, MSCs appeared viable and expressed abundant SMA filaments (Fig. 1B(ii)), which were diminished by PDGFR inhibitor-IV. Compared to control spheroids at day 5, PDGFR inhibitor-IV spheroids expressed 2.9 ± 0.3 -fold lower SMA protein (Fig. 1C).

PDGFR β is known to regulate FN expression [27]. Having shown that PDGFR inhibitor-IV spheroids contained markedly reduced SMA and FN, we used siRNA knockdown to investigate how FN influences the fate of MSCs within 3D spheroids. Compared to spheroids formed from scrambled siRNA knockdown MSCs, spheroids assembled by FN knockdown MSCs displayed a $79\% \pm 9\%$ reduction in FN protein (Fig. 1D) expression, respectively, by day 5 of culture. Like the PDGFR inhibitor-IV treated spheroids (Fig. 1A), these FN knockdown spheroids had larger diameters than control spheroids (Fig. 1E). The FN knockdown MSCs also appeared more rounded and in closer contact than control cells and, compared to scrambled siRNA knockdown spheroids, they expressed markedly reduced SMA filaments (Fig. 1B(iii)) and had a $70\% \pm 8\%$ decrease in SMA protein expression (Fig. 1F). FN knockdown spheroids also displayed significantly diminished PDGFR β phosphorylation (Y751 $80\% \pm 7\%$ and Y1021 $85\% \pm 8\%$ reduction, respectively) (Fig. 1G, 1H). These data show that PDGFRs, and FN which activates PDGFRs, both regulate SMA contractile filaments and coordinate MSC spheroid organization and contractility.

PDGFR Inhibition and FN Depletion Increase Oct4A and Nanog Expression

Having shown that PDGFR inhibition and FN knockdown altered MSC organization within 3D spheroids, we determined their effects on expression of the pluripotency markers Oct4A and Nanog. Compared to untreated adherent MSCs, control spheroids increased Oct4A (5.5 ± 0.6 -fold) and Nanog (6.4 ± 0.5 -fold) transcript levels, and PDGFR inhibitor-IV spheroids further increased Oct4A (10.4 ± 0.8 -fold) and Nanog (11.0 ± 0.7 -fold) (Fig. 2A). To compare these transcript levels with those expressed by pluripotent human embryonic stem cells (ESCs), we examined levels of Oct4A and Nanog expressed by a human ESC line Hues1 (Fig. 2B). Compared to control spheroids, PDGFR inhibitor-IV spheroids increased Oct4A (2.1 ± 0.2 -fold) and Nanog (2.2 ± 0.2 -fold), while ESCs demonstrated a greater level of Oct4A (5.3 ± 0.4 -fold) and Nanog (4.6 ± 0.4 -fold). Oct4A and Nanog transcript expression increased throughout the 5-day culture in both control and PDGFR inhibitor-IV-treated spheroids, with the PDGFR inhibitor-IV spheroids producing the greater increase (Fig. 2C).

Immunofluorescence analysis revealed no Oct4A and a low abundance of Nanog within day 5 control spheroids (Fig. 2D). In contrast, Nanog and Oct4A were initially detected at day 3 and day 1, respectively, in PDGFR inhibitor-IV spheroids (Supporting Information Fig. S1), and both factors increased in abundance up to day 5 (Fig. 2D). Both Nanog and Oct4A expression were dependent on Janus kinase (JAK) signaling (Supporting Information Fig. S2A, S2B), while nuclear STAT3 (Y705) and STAT1 (Y701) increased markedly within PDGFR inhibitor-IV spheroids (Supporting Information Fig. S2C). Compared to control spheroids at day 5, PDGFR inhibitor-IV spheroids expressed significantly higher levels of both Oct4A (3.3 ± 0.3 -fold) (Fig. 2F) and Nanog (3.0 ± 0.2 -fold) protein (Fig. 2G), which were JAK signaling-dependent (Supporting Information Fig. S2D).

Immunofluorescence analysis revealed that, while there was no detectable Oct4A, and low Nanog expression within day 5 scrambled knockdown spheroids, FN knockdown spheroids markedly increased Nanog and Oct4A expression (Fig. 2E). Immunoblot

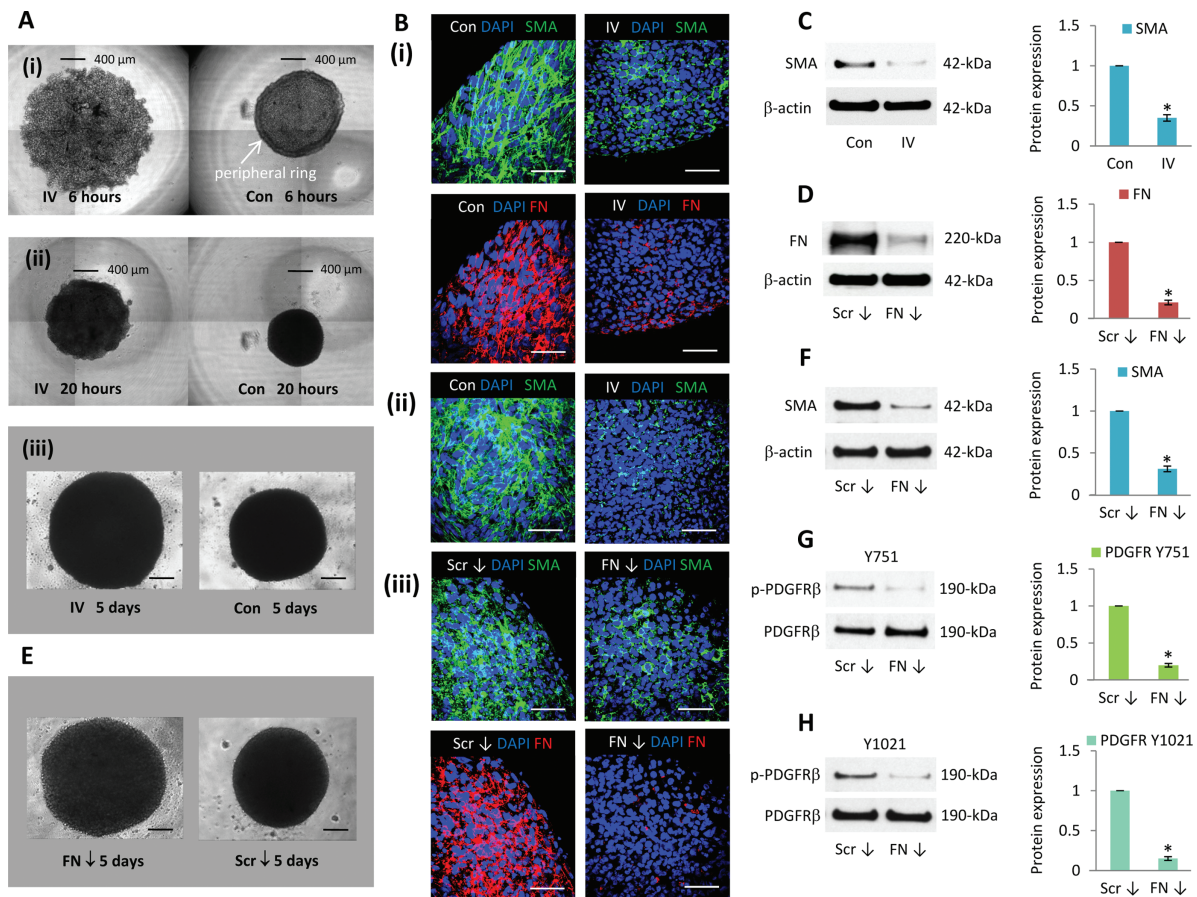


Figure 1. PDGFR and FN inhibition changed mesenchymal stromal/stem cell (MSC) spheroid shape and SMA expression. **(A):** Bright-field images of control and PDGFR inhibitor-IV treated MSCs during spheroid assembly, showing cells (i) 6 hours, (ii) 20 hours, and (iii) 5 days following seeding. Scale bars = 400 μ m (i, ii) and 200 μ m (iii). **(B):** Whole mount immunofluorescence analysis of (i, ii) control spheroids (con) and PDGFR inhibitor-IV spheroids (IV), (iii) scrambled control siRNA spheroids (Scr ↓) and FN knockdown spheroids (FN ↓) cultured for 5 days, showing FN (red) and SMA (green) expression, with DAPI-stained nuclei (blue). Scale bars = 50 μ m. **(C):** Immunoblot analysis of SMA expression within control (Con) and PDGFR inhibitor-IV (IV) spheroids after 5 days culture, with β -actin as a loading control. Histogram shows SMA expression relative to β -actin and normalized to control spheroid level. *, $p < .001$ compared with day 5 control spheroids, using paired t test $n = 3$ separate experiments, error bars represent SD. **(D):** Immunoblot analysis of FN expression within control scrambled siRNA spheroids (Scr ↓) and FN knockdown spheroids (FN ↓) cultured for 5 days, with β -actin as a loading control. RNA expression is relative to GAPDH and normalized to the level of scrambled control spheroids at day 5. Histogram shows protein expression relative to β -actin and normalized to control siRNA spheroid level. *, $p < .001$ compared with control siRNA spheroids, using paired t test $n = 3$ separate experiments, error bars represent SD. **(E):** Bright-field images of spheroids assembled with MSCs treated with scrambled (Scr) or FN small interfering RNAs (siRNA) and cultured for 5 days. Scale bars = 200 μ m. **(F–H):** Immunoblot analysis of SMA, PDGFR β Y751, and Y1021 phosphorylation levels, within scrambled control siRNA spheroids (Scr ↓) and FN knockdown spheroids (FN ↓) after 5 days culture, with β -actin or PDGFR β as a loading control. Histograms show SMA expression relative to β -actin and PDGFR β Y751 and Y1021 relative to PDGFR β , normalized to scrambled control siRNA spheroid level. *, $p < .001$ compared with control spheroids, using paired t test $n = 3$ separate experiments, error bars represent SD. Abbreviations: FN, fibronectin; PDGFR, platelet-derived growth factor receptor.

analysis also confirmed an increase in Oct4A (2.1 ± 0.2 -fold) (Fig. 2H) and Nanog (2.5 ± 0.3 -fold) (Fig. 2I), although these levels were lower than in the PDGFR inhibitor-IV spheroids.

Thus, in comparison to adherent MSC cultures, spindle-shaped MSCs within 3D control spheroids increased the expression of Oct4A and Nanog transcripts, although only low levels of protein were detected. However, inhibition of PDGFR signaling or FN knockdown within spheroids, which induced more rounded MSCs, prominently upregulated Oct4A and Nanog protein levels.

MSC Spheroids Display a Mesendoderm Expression Profile

Having established that MSCs cultured as 3D spheroids markedly upregulate the expression of the pluripotency transcrip-

tion factors Nanog and Oct4A, we investigated expression levels of mesendoderm and endoderm transcription factors expressed by spheroids at day 5 (Fig. 3). Bipotent mesendoderm cells are precursors for both endoderm and mesoderm during ESC differentiation [31]. Mesendoderm has been characterized as Gsc^+ E-cadherin (CDH1) $^+$ PDGFR α^+ which can give rise to Gsc^+ CDH1 $^+$ PDGFR α^- endoderm and Gsc^+ CDH1 $^-$ PDGFR α^+ mesoderm progenitors [31]. Compared to untreated adherent MSCs, control spheroids expressed increased transcripts of mesendoderm transcription factors; Nodal, Mixl, EOMES, Foxh1, and Gsc (Fig. 3A), but PDGFR inhibitor-IV spheroids expressed higher levels of Mixl, EOMES, and Foxh1 (Fig. 3A). Control spheroids also expressed increased levels of the endoderm transcription factors; Foxa1,

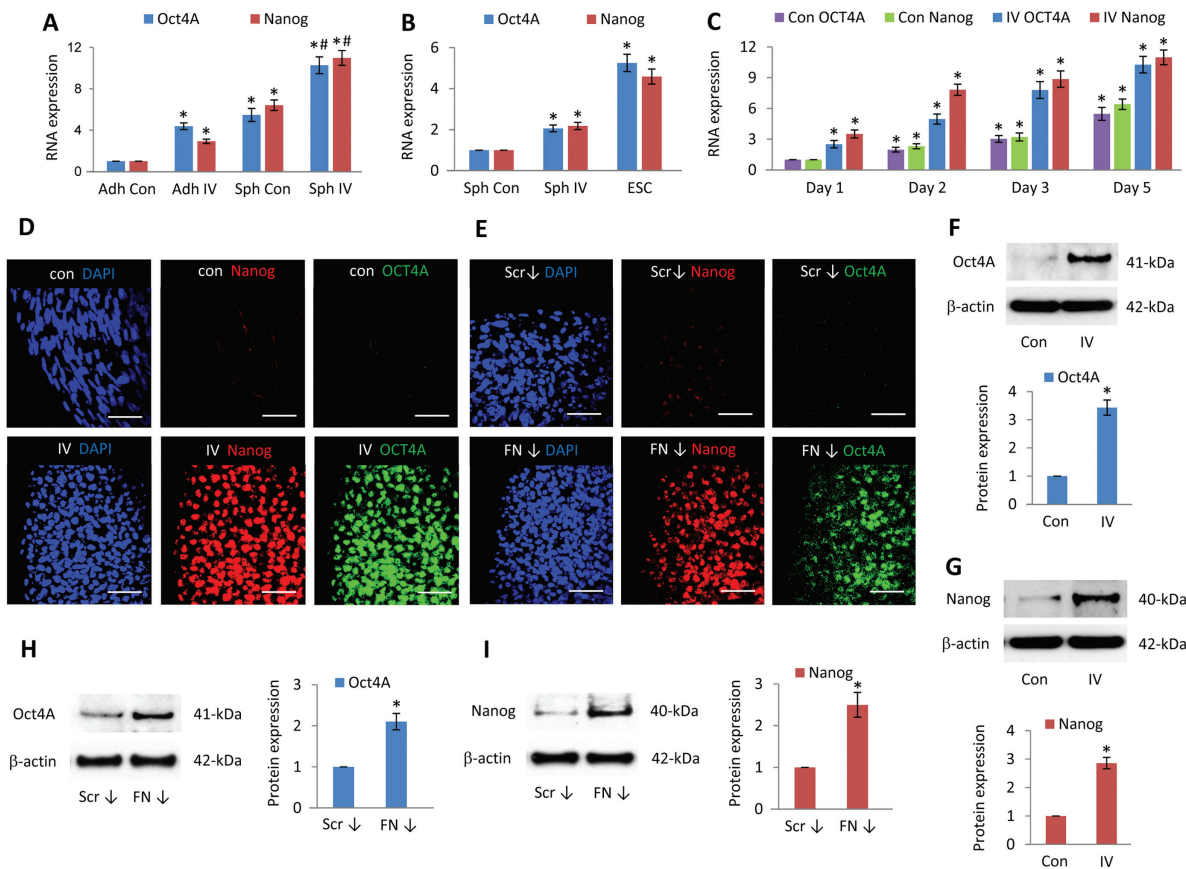


Figure 2. Platelet-derived growth factor receptor (PDGFR) and fibronectin (FN)-inhibited spheroids upregulate Oct4A and Nanog. **(A):** Quantitative RT-PCR analysis of Oct4A and Nanog expression within high-density adherent mesenchymal stromal/stem cells (MSCs) (Adh Con), high-density adherent MSCs exposed to PDGFR inhibitor-IV (Adh IV), control spheroids (Sph Con), and PDGFR inhibitor-IV spheroids (Sph IV), cultured for 5 days. Data are relative to GAPDH and normalized to adherent control levels. *, $p < .001$ compared with adherent controls, #, $p < .001$ compared with control spheroids, using paired t test $n = 3$ separate experiments, error bars represent SD. **(B):** Quantitative RT-PCR analysis of Oct4A and Nanog expression within control spheroids (Sph Con) and PDGFR inhibitor-IV spheroids (Sph IV), cultured for 5 days, and human embryonic stem cell line Hues1. Data are relative to GAPDH and normalized to control spheroid levels. *, $p < .001$ compared with control spheroids, using paired t test $n = 2$ separate experiments, error bars represent SD. **(C):** Quantitative RT-PCR analysis of Oct4A and Nanog expression within control spheroids (Con) and PDGFR inhibitor-IV spheroids (IV), cultured for 1, 2, 3, and 5 days. Data are relative to GAPDH and normalized to the level of control spheroids at day 1. *, $p < .001$ compared with day 1 control spheroids, using paired t test $n = 3$ separate experiments, error bars represent SD. **(D, E):** Whole mount immunofluorescence analysis of (D) control spheroids (Con) and PDGFR inhibitor-IV spheroids (IV), (E) scrambled control siRNA spheroids (Scr ↓), and FN knockdown spheroids (FN ↓) cultured for 5 days, showing Nanog (red) and Oct4A (green) expression, with DAPI-stained nuclei (blue). Scale bars = 50 μ m. **(F–I):** Immunoblot analysis of Oct4A and Nanog expression within (F, G) control (Con) and PDGFR inhibitor-IV (IV) spheroids and (H, I) scrambled control siRNA spheroids (Scr ↓) and FN knockdown spheroids (FN ↓) after 5 days culture, with β -actin as a loading control. Histograms show Oct4A and Nanog expression relative to β -actin and normalized to control spheroid or scrambled control siRNA control spheroid levels. *, $p < .001$ compared with control spheroids, using paired t test $n = 3$ separate experiments, error bars represent SD.

Foxa2, α -fetoprotein (AFP), and Sox17 (Fig. 3B), which were further increased in PDGFR inhibitor-IV spheroids (Fig. 3B).

We therefore examined the expression of the definitive endoderm marker CDH1 [32], which is essential for maintaining ESC pluripotency [33] and is implicated in iPS cell generation [34]. Compared to untreated adherent MSCs, control spheroids expressed increased CDH1 (2.8 ± 0.4 -fold) transcript; however, levels of mesoderm markers CDH2, SMA, and vimentin remained similar (Fig. 3C). In contrast, PDGFR inhibitor-IV spheroids expressed significantly higher CDH1 (4.5 ± 0.2 -fold), whereas levels of CDH2, SMA, and vimentin were markedly decreased (Fig. 3C). Compared to control spheroids, PDGFR inhibitor-IV spheroids showed an increase of

1.8 ± 0.1 -fold in CDH1 transcript, while human ESCs demonstrated a higher level (4.1 ± 0.3 -fold) (Fig. 3D). Immunofluorescence analysis revealed no detectable CDH1 protein within control spheroids (Fig. 3E), but CDH1 protein was readily detected and characteristically localized at cell-cell boundaries within PDGFR inhibitor-IV spheroids (Fig. 3E).

To investigate further the increased expression of pluripotency and endoderm proteins within PDGFR inhibitor-IV spheroids, a stem cell proteome array was used to detect relative expression levels simultaneously (Supporting Information Fig. S3A). Compared to control spheroids, PDGFR inhibitor-IV spheroids showed a distinct increase in the pluripotent markers; Oct4, Nanog, and Sox2, and endoderm markers; Sox17, AFP,

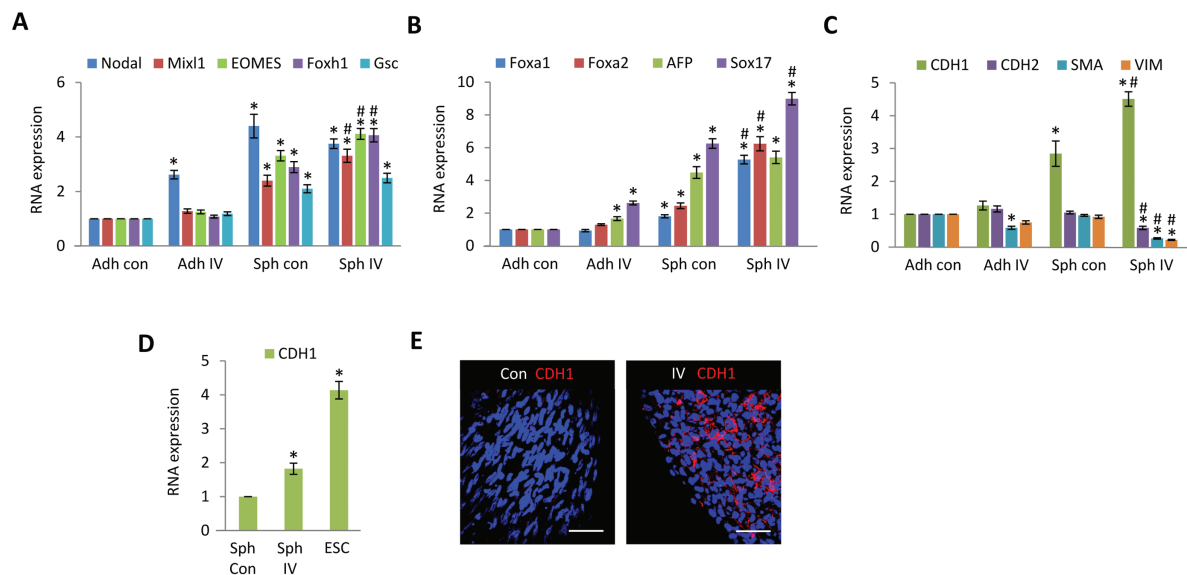


Figure 3. Platelet-derived growth factor receptor (PDGFR)-inhibited spheroids express E-cadherin. **(A–C):** Quantitative RT-PCR analysis of (A) Nodal, Mixl1, EOMES, Foxh1, and Goosecoid (Gsc) (B) Foxa1, Foxa2, AFP, and Sox17, (C) E-cadherin (CDH1), N-cadherin (CDH2), SMA, and vimentin (VIM), within high-density adherent mesenchymal stromal/stem cells (MSCs) (Adh con), high-density adherent MSCs exposed to PDGFR inhibitor-IV (Adh IV), control spheroids (Sph con), and PDGFR inhibitor-IV spheroids (Sph IV), cultured for 5 days. Data are relative to GAPDH and normalized to adherent control levels. *, $p < .001$ compared with adherent controls, #, $p < .005$ compared with control spheroids, using paired t test $n = 3$ separate experiments, error bars represent SD. **(D):** Quantitative RT-PCR analysis of CDH1 within control spheroids (Sph Con) and PDGFR inhibitor-IV spheroids (Sph IV), cultured for 5 days, and human ESC line Hues1. Data are relative to GAPDH and normalized to control spheroid levels. *, $p < .001$ compared with spheroid controls, using paired t test $n = 2$ separate experiments, error bars represents SD. **(E):** Whole mount immunofluorescence analysis of control spheroids (con) and PDGFR inhibitor-IV spheroids (IV) cultured for 5 days, showing CDH1 (red) expression with DAPI-stained nuclei (blue). Scale bars = 50 μm. Abbreviations: AFP, α -fetoprotein; ESC, embryonic stem cell.

Foxa2, and CDH1. These data verify that PDGFR inhibitor-IV spheroids express mesendoderm and endoderm markers including CDH1, indicating features of a mesendoderm progenitor.

Proteome array analysis demonstrated that, compared to scrambled siRNA knockdown spheroids, FN knockdown spheroids also upregulated Oct4, Nanog, and Sox2 as well as endoderm markers; Sox17, AFP, Foxa2, and CDH1 (Supporting Information Fig. S3B). Thus, FN knockdown also resulted in features of a mesendoderm progenitor, although the relative levels of these markers were lower than those induced by PDGFR inhibition (Supporting Information Fig. S3A). These data indicate that inhibition of PDGFR signaling, or FN depletion, within spheroids reverts MSCs toward a more multipotent state.

MSC Spheroids Exhibit Endothelial Characteristics

Using mesoderm progenitor cells derived from ESCs, activation of PDGFR β signaling can induce differentiation to vascular smooth muscle cells, which express abundant SMA, whereas stimulation with VEGF-A can induce differentiation toward endothelial cells [35]. In addition, adherent MSCs cultured in two-dimensional (2D) at high density acquire a more rounded cobblestone-like morphology, and can undergo differentiation toward an endothelial lineage [9]. We therefore explored the possibility that MSCs within PDGFR inhibitor-IV spheroids, which lack PDGFR signaling, have depleted SMA and are at high density, may exhibit an endothelial rather than mesenchymal disposition. Accordingly, the expression of two characteristic endothelial markers, PECAM-1 and VE-cadherin, was determined in PDGFR inhibitor-IV spheroids.

Compared to untreated adherent MSCs, control spheroids expressed significantly increased PECAM-1 (6.7 ± 0.7 -fold) and VE-cadherin (6.4 ± 0.6 -fold) transcript levels (Fig. 4A). However, compared to control spheroids, PDGFR inhibitor-IV spheroids expressed an even higher level of PECAM-1 (2.1 ± 0.23 -fold) and VE-cadherin (1.6 ± 0.17 -fold) (Fig. 4A). Control spheroids increased the level of both PECAM-1 and VE-cadherin transcripts up to day 5, while PDGFR inhibitor-IV spheroids produced a greater increase (Fig. 4B). Immunofluorescence analysis revealed that control spheroids, which contained spindle-shaped MSCs, expressed both PECAM-1 and VE-cadherin protein, which increased up to day 5 (Fig. 4C and Supporting Information Fig. S4A). Similarly, PDGFR inhibitor-IV spheroids, which contained more rounded MSCs, displayed prominent PECAM-1 and VE-cadherin expression, but in this case the protein appeared localized around individual cells (Fig. 4D and Supporting Information Fig. S4B). Compared to control spheroids at day 5, PDGFR inhibitor-IV spheroids significantly expressed a higher level of PECAM-1 protein (2.4 ± 0.2 -fold) (Fig. 4E), which was JAK signaling dependent (Supporting Information Fig. S2D–S2F). Compared to PDGFR inhibitor-IV spheroids, human umbilical vein endothelial cells (HUVECs) expressed a greater level of PECAM-1 (2.7 ± 0.4 -fold).

FN knockdown spheroids, which caused similar effects on cell shape and phenotype (Fig. 1), increased PECAM-1 protein (1.9 ± 0.17 -fold) (Fig. 4F). The effects of EGFR, FGFR, VEGFR, ROK, Rac, MEK, or PI3K signaling inhibitors on PECAM-1 and VE-cadherin transcripts were also examined, but only ROK or Rac inhibition markedly increased PECAM-1 expression (Fig. 4G). Rac or ROK-inhibited spheroids were shown to increase

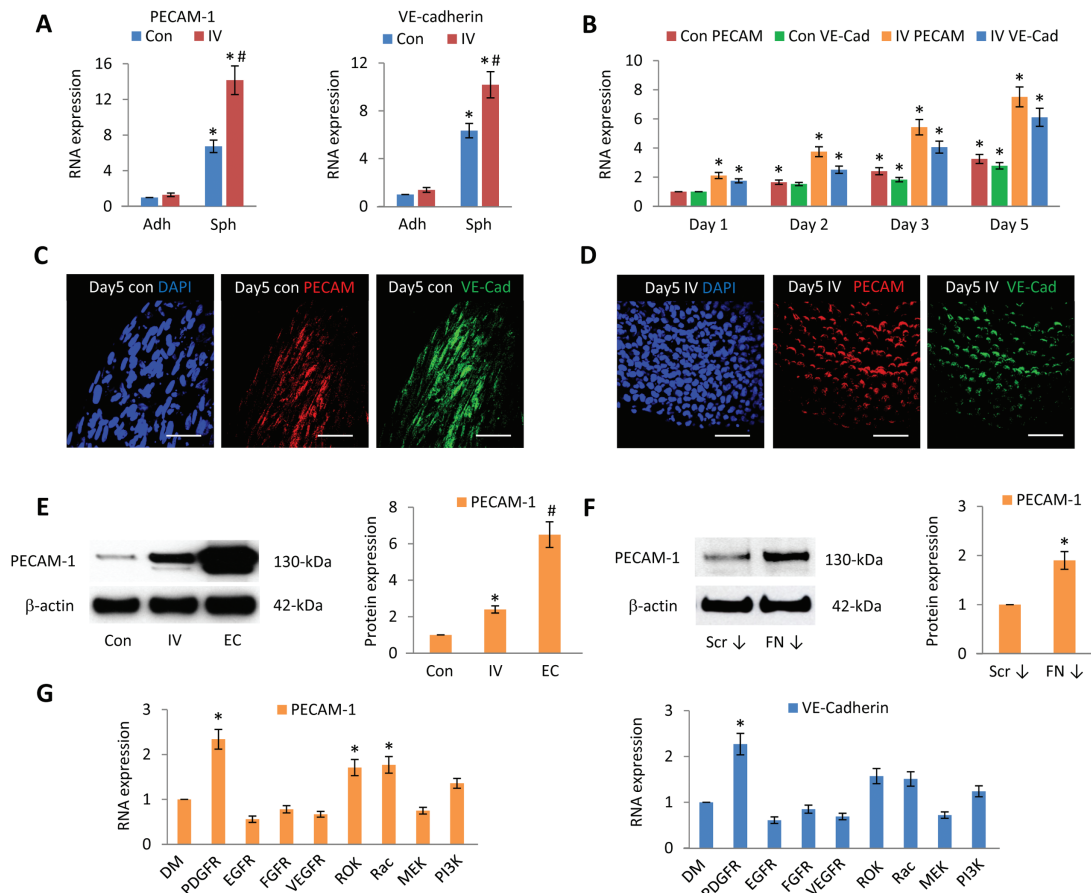


Figure 4. PDGFR and FN-inhibited spheroids upregulate endothelial markers. **(A):** Quantitative RT-PCR analysis of PECAM-1 and VE-cadherin expression within high-density adherent mesenchymal stromal/stem cells (MSCs) (Adh Con), high-density adherent MSCs exposed to PDGFR inhibitor-IV (Adh IV), control spheroids (Sph Con), and PDGFR inhibitor-IV spheroids (Sph IV), cultured for 5 days. Data are relative to GAPDH and normalized to adherent control levels. *, $p < .001$ compared with adherent controls, #, $p < .001$ compared with control spheroids, using paired t test $n = 3$ separate experiments, error bars represent SD. **(B):** Quantitative RT-PCR analysis of PECAM-1 and VE-cadherin expression within control spheroids (Con) and PDGFR inhibitor-IV spheroids (IV), cultured for 1, 2, 3, and 5 days. Data are relative to GAPDH and normalized to the level of control spheroids at day 1. *, $p < .001$ compared with day 1 control spheroids, using paired t test $n = 3$ separate experiments, error bars represent SD. **(C, D):** Whole mount immunofluorescence analysis of **(C)** control spheroids (con) and **(D)** PDGFR inhibitor-IV spheroids (IV), cultured for 5 days, showing PECAM-1 (red) and VE-cadherin (green) expression, with DAPI-stained nuclei (blue). Scale bars = 50 μ m. **(E, F):** Immunoblot analysis of PECAM-1 expression within control (Con), PDGFR inhibitor-IV (IV) spheroids, HUVECs (EC) and control scrambled siRNA spheroids (Scr ↓), and FN knockdown spheroids (FN ↓) after 5 days culture, with β -actin as loading control. Histogram shows PECAM-1 expression relative to β -actin and normalized to control spheroid or control siRNA spheroid levels. *, $p < .001$ compared with control spheroids, #, $p < .001$ compared with PDGFR inhibitor-IV spheroids, using paired t test $n = 3$ separate experiments, error bars represent SD. **(G):** Quantitative RT-PCR analysis of PECAM-1 and VE-cadherin expression within control spheroids, cultured for 5 days in the presence of DMSO (DM) carrier, or 0.1 μ M PDGFR inhibitor-IV, 2 nM EGFR, 0.1 μ M FGFR, 0.5 μ M VEGFR, 5 nM ROK, 50 μ M Rac1, 20 μ M MEK, or 5 μ M PI3K inhibitors. Data are relative to GAPDH and normalized to DMSO treated spheroid levels. *, $p < .001$ compared with control spheroids, using paired t test $n = 3$ separate experiments, error bars represent SD. Abbreviations: FN, fibronectin; PDGFR, platelet-derived growth factor receptor.

PECAM-1 protein (1.63 ± 0.13 -fold and 1.68 ± 0.15 -fold, respectively) (Supporting Information Fig. S4C); however, this level was lower than that expressed by PDGFR inhibitor-IV or FN-depleted spheroids.

MSC Spheroids Secrete Angiogenic Factors

To identify proteins secreted by MSC spheroids which may regulate the endothelial features identified, we used a human angiogenesis proteome array to analyze supernatants from adherent 2D MSCs at high density, or 3D MSC spheroids, cultured in the presence or absence of PDGFR inhibitor-IV for 3 days (Fig. 5).

Compared to adherent controls, both control and PDGFR-IV spheroids prominently upregulated the secretion of activin-A, ADAMTS-1, dipeptidyl peptidase-4, EGF, endostatin, FGF-1, glial cell line-derived neurotrophic factor, IGFBP-1, IL-8, PIGF, and VEGF-C, but downregulated the secretion of angiopoietin-1, FGF-7, monocyte chemoattractant protein-1, and thrombospondin-1. Compared to control spheroids, PDGFR-IV spheroids secreted higher levels of ADAMTS-1 (1.5 ± 0.12 -fold), endoglin (1.5 ± 0.13 -fold), FGF-1 (1.6 ± 0.11 -fold), HGF (1.7 ± 0.13 -fold), vasohibin (1.5 ± 0.12 -fold), and VEGF-C (1.3 ± 0.09 -fold), but markedly decreased the secretion of amphiregulin (3.9 ± 0.3 -fold), IL-8 (1.5 ± 0.12 -fold), and leptin (2.5 ± 0.2 -fold). A list of

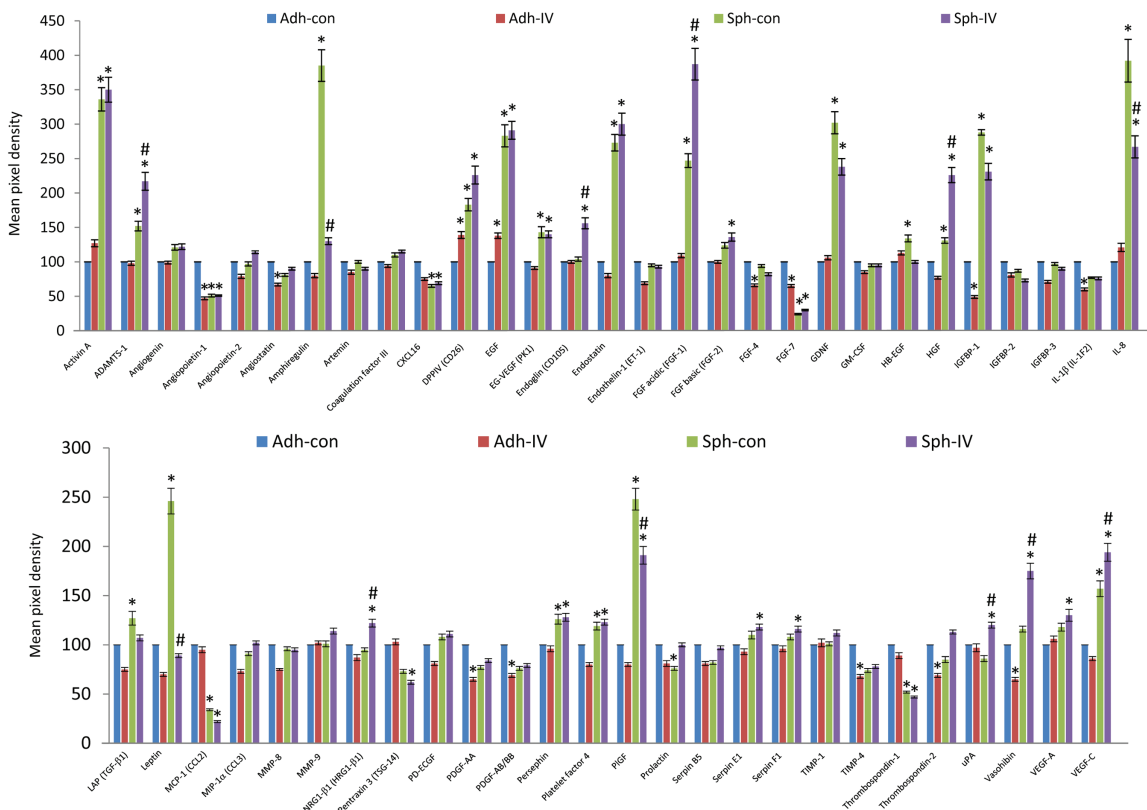


Figure 5. Angiogenic factors secreted by mesenchymal stromal/stem cell (MSC) spheroids. A human angiogenesis array kit (ARY007) (R&D Systems, Minneapolis, MN, <http://www.rndsystems.com>) was used to determine simultaneously the relative expression levels of 55 different angiogenic proteins, secreted by high-density adherent MSCs (Adh Con), high-density adherent MSCs exposed to PDGFR inhibitor-IV (Adh IV), control spheroids (Sph Con), and PDGFR inhibitor-IV spheroids (Sph IV), cultured for 3 days. Prior to analysis, adherent MSCs and spheroids were cultured for 2 days, then fresh growth medium added and cultured for a further 3 days for analysis. Supernatants from 24 identical adherent or spheroid cultures were pooled for analysis. Data are normalized to the DNA content of each MSC culture, and relative to high-density adherent MSCs (Adh con) *, $p < .001$ compared with adherent controls, #, $p < .005$ compared with control spheroids, using paired t test $n = 1$ experiment, error bars represent SD between two repeats.

the relative expression levels of all 55 secreted proteins is given in Supporting Information Table S3.

Taken together, these data demonstrate that the 3D culture of MSCs as spheroids markedly increased the secretion of potent angiogenic-related proteins, and dramatically upregulated the expression of PECAM-1 and VE-cadherin transcripts, compared with 2D culture of MSCs at high density. Furthermore, PDGFR inhibitor-IV and FN-depleted spheroids displayed an increase in PECAM-1 protein when compared with control spheroids, indicating that inhibition of mesenchymal drivers is a primary determinant in the acquisition of these endothelial features.

MSC Spheroids Facilitate Blood Vessel Formation Within Matrigel

Endothelial cells form capillary-like network structures when cultured on Matrigel [36]. We therefore tested the ability of MSCs which had been cultured as spheroids, to form similar Matrigel-induced networks. Control and PDGFR inhibitor-IV spheroids were cultured for 5 days, then MSCs dissociated into single cells and cultured on Matrigel under identical conditions (i.e., no PDGFR inhibitor-IV added) for a further 2 days. PECAM-1 and VE-cadherin expressions were then determined by immunofluorescence analysis (Fig. 6A, 6B). MSCs derived from control spheroids readily established network

structures with elongated branch points. These networks were composed of spindle-shaped cells which expressed both PECAM-1 and VE-cadherin (Fig. 6A). However, some cells expressed neither PECAM-1 nor VE-cadherin (Fig. 6A (ii, iv)). Similarly MSCs derived from PDGFR inhibitor-IV spheroids also readily formed widespread network structures, but in contrast, these had short branch points and the networks were composed of rounded cells, surrounded by distinctive PECAM-1 and VE-cadherin expression (Fig. 6B). Notably in this case, from >25 different images captured, every cell was positive for both PECAM-1 and VE-cadherin (Fig. 6B (ii-iv)).

As a prelude to examining the effects of MSC spheroids on angiogenesis *in vivo*, we cultured MSC spheroids within a 3D Matrigel plug *in vitro*. Control and PDGFR inhibitor-IV spheroids were cultured for 5 days. The intact spheroids were then implanted into Matrigel and cultured under identical conditions (i.e., no PDGFR inhibitor IV added) for a further 5 days. Control spheroids rapidly developed outgrowths of spindle-shaped cells by day 1, which became extensive by day 5 (Fig. 6C). These cellular outgrowths were negative for PECAM-1 and VE-cadherin (Fig. 6D (i-ii)), but positive for SMA (Fig. 6D (iii)). In contrast, PDGFR inhibitor-IV spheroids developed a ring of nonmigratory rounded cells around the spheroid periphery (Fig. 6E), which exhibited abundant PECAM-1 and VE-cadherin expression (Fig.

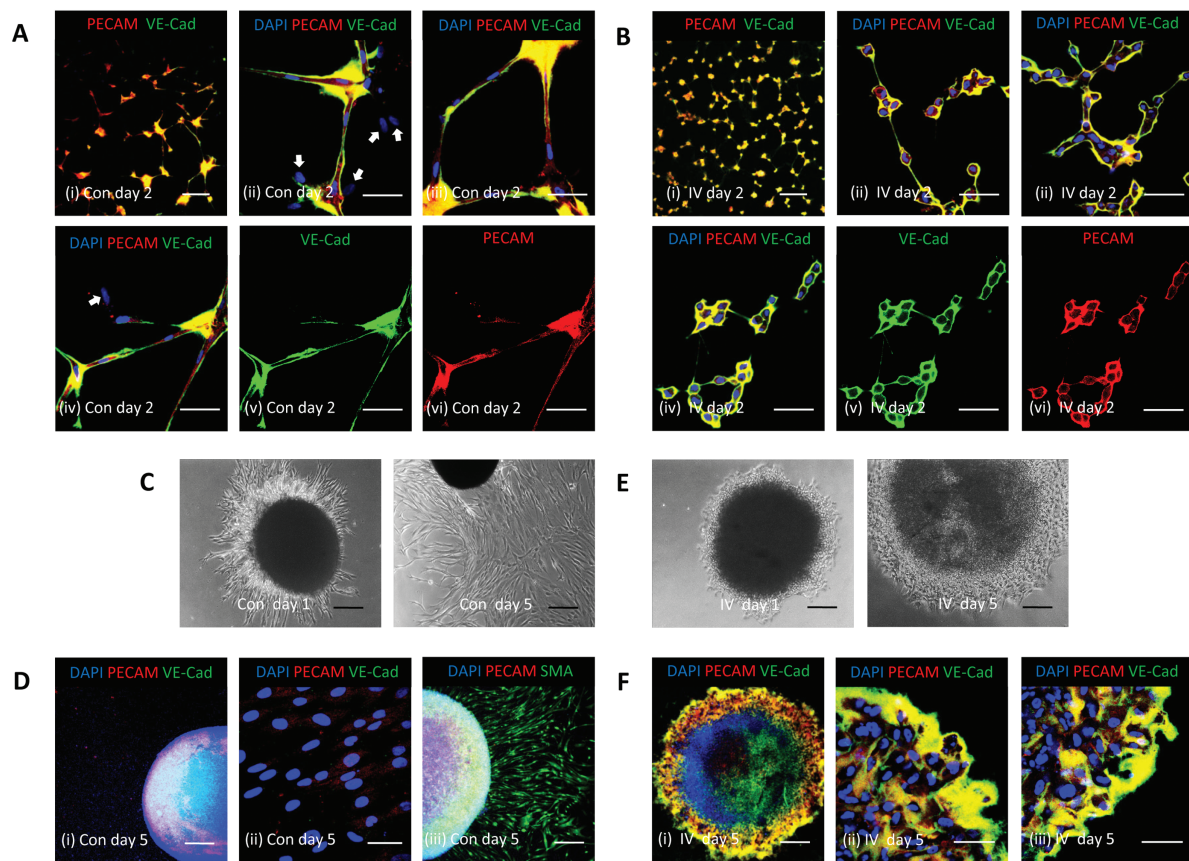


Figure 6. Spheroid-derived platelet-derived growth factor receptor (PDGFR)-inhibited mesenchymal stromal/stem cells (MSCs) form Matrigel-induced networks. **(A, B):** Immunofluorescence analysis of MSCs cultured as spheroids for 5 days, then dissociated into single cells (2×10^4) and cultured on glass coverslips (13-mm diameter) coated with a thin layer of growth factor reduced Matrigel for a further 2 days. **(A)** MSCs derived from control spheroids (Con) and **(B)** MSCs derived from PDGFR inhibitor-IV spheroids (IV), showing network formation and PECAM-1 (red) and VE-cadherin (green) expression, with DAPI-stained nuclei (blue). Image (iv) is shown split into individual channels (v) green (VE-cadherin) and (vi) red (PECAM-1). Arrows in images A (ii, iv) represent MSCs lacking either PECAM-1 or VE-cadherin. Scale bars = 200 μm (i) and 50 μm (ii-vi). **(C, E):** Bright-field images of **(C)** control spheroids (Con) and **(E)** PDGFR inhibitor-IV spheroids (IV), implanted into Matrigel and cultured for 1 day and 5 days. Scale bars = 200 μm . **(D, F):** Whole mount immunofluorescence analysis of **(D)** control spheroids (Con) and **(F)** PDGFR inhibitor-IV spheroids (IV), implanted into Matrigel and cultured for 5 days, showing PECAM-1 (red) and VE-cadherin (green) expression and **(D (iii))** SMA (green) expression, with DAPI-stained nuclei (blue). Scale bars = 200 μm (i) (D (iii)) and 50 μm (ii) (F (iii)).

6F). Live cell imaging was also used to monitor the formation of cellular outgrowths from control spheroids and the peripheral ring of cells around PDGFR inhibitor-IV spheroids, during the first 90 hours of culture within Matrigel (Supporting Information Video S2).

PDGFR-Inhibited MSCs Integrate with Functional *In Vivo* Blood Vessels

To determine the effects of MSC spheroids on *in vivo* angiogenesis, 10 control or PDGFR inhibitor-IV spheroids were suspended in Matrigel without any additional growth factors, and implanted into mice for 14 days, then human and murine PECAM-1 expression determined by immunofluorescence (Fig. 7). In addition, new functional blood vessels connected to the circulation were identified by FITC-dextran perfusion.

Examination of excised Matrigel plugs revealed that the control spheroids contained few human PECAM-1 positive cells present (Fig. 7A), but these spheroids were infiltrated by murine PECAM-1 positive blood vessels; the absence of

FITC-dextran staining suggested that these vessels were not attached to the circulation (Fig. 7B). Similarly, the Matrigel surrounding the control spheroids was permeated with murine PECAM-1 positive blood vessels; however, few human PECAM-1-positive cells were observed (Fig. 7B), and these vessels were also not associated with FITC-dextran perfusion (Fig. 7D). Analysis of the peripheral tissue revealed numerous blood vessels (Fig. 7C), but only minimal human PECAM-1-positive staining was detected (Fig. 7D), which again was not detected near FITC-dextran staining (Fig. 7F).

In marked contrast, PDGFR inhibitor-IV spheroids contained numerous human PECAM-1-positive cells and these spheroids were also infiltrated by murine blood vessels (Fig. 7G), which were connected to the host circulation as indicated by abundant FITC-dextran perfusion (Fig. 7H). The Matrigel surrounding PDGFR inhibitor-IV spheroids was also permeated with both murine and human PECAM-1-positive cells, which associated together in vascular-like assemblies (Fig. 7I). Some of these human PECAM-1-positive vascular-like assemblies within Matrigel were perfused with FITC-dextran

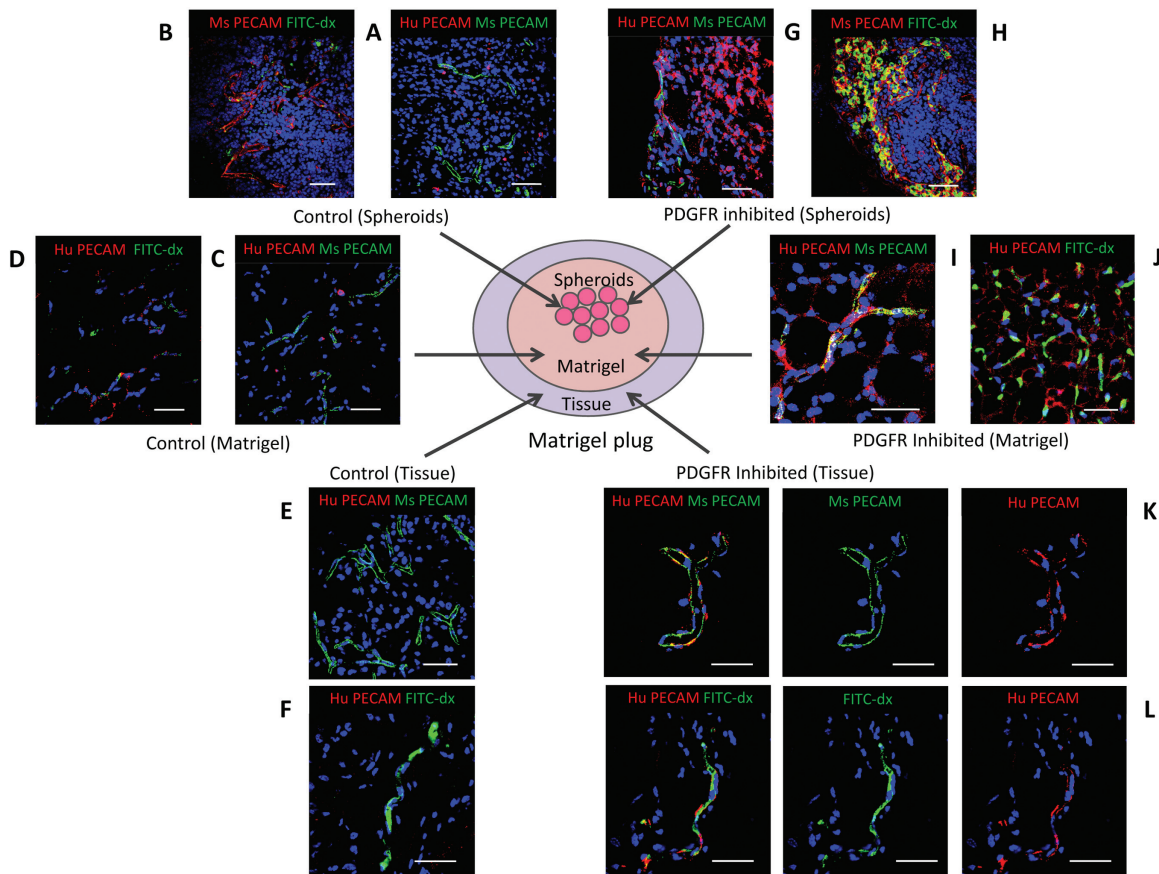


Figure 7. Spheroid-derived platelet-derived growth factor receptor (PDGFR)-inhibited mesenchymal stromal/stem cells integrate with perfused blood vessels. **(A–L):** Immunofluorescence analysis of Matrigel plugs containing control or PDGFR inhibitor-IV spheroids, after implantation in mice for 14 days, showing human (Hu) PECAM-1 (red) and murine (Ms) PECAM-1 (green) expression, or FITC-dextran (FITC-dx) perfusion (green), with DAPI-stained nuclei (blue). Images show representative areas of **(A, B)** control or **(G, H)** PDGFR inhibitor-IV spheroids. Matrigel surrounding **(C, D)** control or **(I, J)** PDGFR inhibitor-IV spheroids. Tissue surrounding **(E, F)** control or **(K, L)** PDGFR inhibitor-IV spheroids. Images **K** and **L** are shown split into their red channel (human PECAM-1) and green channel (murine PECAM-1 or FITC-dextran perfusion). Scale bars = 50 μm .

(Fig. 7J). Human PECAM-1-positive cells derived from PDGFR inhibitor-IV spheroids were also detected in the peripheral tissue, where they clearly integrated into blood vessels with murine PECAM-1 positive cells (Fig. 7K). These human PECAM-1-positive vessels in tissue were connected to the host vasculature and perfused with FITC-dextran (Fig. 7L). Thus, PDGFR inhibitor-IV spheroids are a potent source and stimulant for neovascularization.

DISCUSSION

Mesenchymal cells make tissues by depositing and embedding themselves in an extracellular matrix and growth factor-rich microenvironment, which they remodel and maintain throughout life. Although this extrinsic niche dictates the behavior of MSCs, their therapeutic potential remains severely constrained by lack of mechanistic insight into how the niche controls their fate. Here, we have shown that disrupting the extracellular matrix molecule FN or the functionally linked PDGFR, which together regulate mesenchyme [22], converts MSCs rapidly from SMA-rich spindle-shaped contractile cells to rounded E-cadherin-rich cells. These cells exhibit enhanced

expression of markers for pluripotency, mesendoderm, endoderm, and angiogenic markers, and display potent angiogenic behavior *in vivo*. Thus, blocking natural mesenchymal signals offers an effective strategy for reprogramming mesenchymal cells and for therapeutic revascularization.

We have developed a novel approach to modulate MSC fate that does not require the use of viral vectors or exogenous DNA. Using a spheroid MSC culture model that recapitulates physiological features of a 3D cellular environment and cell-cell interactions, MSCs were induced toward a more multipotent state. Untreated MSCs within spheroids retained their spindle-shape and mesenchymal character with a SMA-rich cytoskeleton and profuse FN matrix. Although culturing MSCs as 3D spheroids was sufficient to induce some upregulation of mesendodermal and endodermal markers, inhibition of PDGFRs or FN knockdown induced rapid cell rounding along with significant further induction of pluripotency markers Oct4A and Nanog, demonstrating that MSCs have the potential to revert to a pre-mesenchymal state, which is accentuated when mesenchymal signals are inhibited. We have previously shown using 2D cultured MSCs that PDGFR signaling inhibition changes their shape and cell fate [28]. In this study, depletion of the extracellular matrix

component FN was also shown to modulate MSC shape and direct their fate, emphasizing the crucial role played by cell shape in MSC fate decisions. Furthermore, we were able to demonstrate that these cells had strong angiogenic potential *in vitro* and *in vivo*. Thus, disrupting mesenchymal signals in these 3D cultures induced a mesenchymoangioblast-like state [3, 4].

It has been unclear whether MSCs possess the ability to transdifferentiate to functional endothelial cells; most reports have relied on exogenous VEGF-A supplementation approaches [8]. We previously showed that high-density cultures exhibited Notch-dependent endothelial potential *in vitro* and in CAM assays [9]. Here, by demonstrating that MSCs derived from PDGFR-inhibited spheroids are able to induce, and integrate with functional blood vessels perfused by the circulation *in vivo*, we have directly shown their angiogenic and vascular potential. By inhibiting mesenchymal signals, we were able to induce endothelial fate, including the reinstigation of robust cell-cell interactions, as judged by E-cadherin expression. Thus cell-cell contacts within PDGFR-inhibited spheroids may be just as important in driving the angiogenic features, as increased expression of embryonic transcription factors.

CONCLUSION

In summary, we have shown that the mesenchymal fate of MSCs can be modulated by re-engineering the relationship

between cells and their local matrix, without the need for viral delivery of exogenous transcription factors. By blocking mesenchymal drivers, these cells can be reverted to a mesenchymoangioblast-like state and thence to functional endothelial-like cells *in vivo*. As these strategies target the natural mechanisms that manipulate mesenchymal fate, they have great potential for future revascularization therapies.

ACKNOWLEDGMENTS

We thank Dr. Mark Travis (Faculty of Life Sciences, University of Manchester, U.K.) for facilitating the *in vivo* study, and David Bolton and Elen Bray (CM Technologies) for assistance with producing the on-line videos. This study was funded by a Strategic Award (G0902170) from the Medical Research Council (U.K.) and British Heart Foundation (Kielty, principal investigator; Canfield and Merry, coinvestigators).

AUTHOR CONTRIBUTIONS

S.G.B.: conception and design, collection and assembly of data, data analysis and interpretation, and manuscript writing; J.J.W.: animal procedures; A.E.C. and C.L.R.M.: manuscript writing; C.M.K.: conception and design, manuscript writing, financial support, and final approval of manuscript.

DISCLOSURE OF POTENTIAL CONFLICTS OF INTEREST

The authors indicate no potential conflicts of interest.

REFERENCES

- Pittenger MF, Mackay AM, Jaiswal RK et al. Multilineage potential of adult human mesenchymal stem cells. *Science* 1999;284:143–147.
- Dominici M, Le Blanc K, Mueller I et al. Minimal criteria for defining multipotent mesenchymal stromal cells. The International Society for Cellular Therapy position statement. *Cytotherapy* 2006;8:315–317.
- Slukvin II, Vodyanik M. Endothelial origin of mesenchymal stem cells. *Cell Cycle* 2011;10:1370–1373.
- Vodyanik MA, Yu J, Zhang X et al. A mesoderm-derived precursor for mesenchymal stem and endothelial cells. *Cell Stem Cell* 2010;7:718–729.
- Crisan M, Yap S, Casteilla L et al. A perivascular origin for mesenchymal stem cells in multiple human organs. *Cell Stem Cell* 2008;3:301–313.
- Méndez-Ferrer S, Michurina TV, Ferraro F et al. Mesenchymal and haematopoietic stem cells form a unique bone marrow niche. *Nature* 2010;466:829–834.
- Bianco P, Cao X, Frenette PS et al. The meaning, the sense and the significance: Translating the science of Mesenchymal stem cells into medicine. *Nat Med* 2013;19:35–42.
- Oswald J, Boxberger S, Jørgensen B et al. Mesenchymal stem cells can be differentiated into endothelial cells *in vitro*. *Stem Cells* 2004;22:377–384.
- Whyte JL, Ball SG, Shuttleworth CA et al. Density of human bone marrow stromal cells regulate commitment to vascular lineages. *Stem Cell Res* 2011;6:238–250.
- Dennis JE, Charbord P. Origin and differentiation of human and murine stroma. *Stem Cells* 2002;20:205–214.
- Morikawa S, Mabuchi Y, Niibe K et al. Development of mesenchymal stem cells partially originate from the neural crest. *Biochem Biophys Res Commun* 2009;379:1114–1119.
- Lee G, Kim H, Elkabetz Y et al. Isolation and directed differentiation of neural crest stem cells derived from human embryonic stem cells. *Nat Biotechnol* 2007;25:1468–1475.
- Minasi MG, Riminucci M, De Angelis L et al. The meso-angioblast: A multipotent self-renewing cell that originates from the dorsal aorta and differentiates into most mesodermal tissues. *Development* 2002;129:2773–2783.
- Betsholtz C, Karlsson L, Lindahl P. Developmental roles of platelet-derived growth factors. *Bioessays* 2001;23:494–507.
- Andrae J, Gallini R, Betsholtz C. Role of platelet-derived growth factors in physiology and medicine. *Genes Dev* 2008;22:1276–1312.
- Tallquist M, Kazlauskas A. PDGF signaling in cells and mice. *Cytokine Growth Factor Rev* 2004;15:205–213.
- Soriano P. The PDGF alpha receptor is required for neural crest cell survival and for normal patterning of the somites. *Development* 2009;124:2691–2700.
- Hellström M, Kalén M, Lindahl P et al. Role of PDGF-B and PDGFR-beta in recruitment of vascular smooth muscle cells and pericytes during embryonic blood vessel formation in the mouse. *Development* 1999;126:3047–3055.
- Boström H, Willetts K, Pekny M et al. PDGF-A signaling is a critical event in lung alveolar myofibroblast development and alveogenesis. *Cell* 1996;85:863–873.
- Yang X, Chrisman H, Weijer CJ. PDGF signalling controls the migration of mesoderm cells during chick gastrulation by regulating N-cadherin expression. *Development* 2008;135:3521–3530.
- Ball SG, Shuttleworth A, Kielty CM. Platelet-derived growth factor receptor alpha is a key determinant of smooth muscle alpha actin filaments in bone marrow-derived mesenchymal stem cells. *Int J Biochem Cell Biol* 2007;39:379–391.
- Veevers-Lowe J, Ball SG, Shuttleworth A et al. Mesenchymal stem cell migration is regulated by fibronectin through $\alpha 5 \beta 1$ -integrin-mediated activation of PDGFR- β and potentiation of growth factor signals. *J Cell Sci* 2011;124:1288–1300.
- Ball SG, Bayley C, Shuttleworth CA et al. Neuropilin-1 regulates platelet-derived growth factor receptor signalling in Mesenchymal stem cells. *Biochem J* 2010;427:29–40.
- White ES, Baralle FE, Muro AF. New insights into form and function of fibronectin splice variants. *J Pathol* 2008;216:1–14.
- White ES, Muro AF. Fibronectin splice variants: Understanding their multiple roles

in health and disease using engineered mouse models. *IUBMB Life* 2011;63:538–546.

26 Astrof S, Crowley D, Hynes RO. Multiple cardiovascular defects caused by the absence of alternatively spliced segments of fibronectin. *Dev Biol* 2007;311:11–24.

27 Hewitt KJ, Shamis Y, Knight E et al. PDGFR β expression and function in fibroblasts derived from pluripotent cells is linked to DNA demethylation. *J Cell Sci* 2012;125:2276–2287.

28 Ball SG, Shuttleworth A, Kielty CM. Inhibition of platelet-derived growth factor receptor signaling regulates Oct4 and Nanog expression, cell shape, and mesenchymal stem cell potency. *Stem Cells* 2012;30:548–560.

29 Weiswald LB, Guinebreti re JM, Richon S et al. In situ protein expression in tumour spheres: Development of an immunostaining protocol for confocal microscopy. *BMC Cancer* 2010;10:106.

30 Owens GK. Regulation of differentiation of vascular smooth muscle cells. *Physiol Rev* 1995;75:487–517.

31 Tada S, Era T, Furusawa C et al. Characterization of mesendoderm: A diverging point of the definitive endoderm and mesoderm in embryonic stem cell differentiation culture. *Development* 2005;132:4363–4374.

32 Larue L, Antos C, Butz S et al. A role for cadherins in tissue formation. *Development* 1996;122:3185–3194.

33 Redmer T, Diecke S, Grigoryan T et al. E-cadherin is crucial for embryonic stem cell pluripotency and can replace OCT4 during somatic cell reprogramming. *EMBO Rep* 2011;12:720–726.

34 Chen T, Yuan D, Wei B et al. E-cadherin-mediated cell-cell contact is critical for induced pluripotent stem cell generation. *Stem Cells* 2010;28:1315–1325.

35 Yamashita J, Itoh H, Hirashima M et al. Flk1-positive cells derived from embryonic stem cells serve as vascular progenitors. *Nature* 2000;408:92–96.

36 Ponce ML. Tube formation: An *in vitro* matrigel angiogenesis assay. *Methods Mol Biol* 2009;467:183–188.



See www.StemCells.com for supporting information available online.